



---

**High resolution monitoring, real time visualization  
and reliable modeling of highly controlled,  
intermediate and up-scalable size pilot injection  
tests of underground storage of CO<sub>2</sub>**

**Contract #309067**

<b>Deliverable Number Title</b>	<b>D5.3  Report on the effectiveness of different injection geometries</b>
<b>Work-Package</b>	<b>5</b>
<b>Lead Participant Contributors</b>	<b>CSIC UU, EWRE</b>
<b>Version:</b>	<b>1</b>
<b>Revision level:</b>	<b>01</b>
<b>Due Date:</b>	<b>Month 36</b>
<b>Reviewed by:</b>	
<b>Status:</b>	
<b>Dissemination level</b>	<b>PU</b>

## Executive summary

In this deliverable, we discuss the effectiveness of different injection geometries.

We first present in this report, the effect of the penetration of the injection well into the host reservoir on the CO<sub>2</sub> injection pressure evolution and the CO<sub>2</sub> plume shape. We evaluated two different cases: one with isotropic reservoir permeability and another one with an anisotropic reservoir permeability (vertical permeability one tens of the horizontal one).

Then, we discuss the impact of CO<sub>2</sub> injection through horizontal or vertical wells. For both cases, we evaluated the reservoir overpressure and the aquifer and caprock mechanical stability. This injection geometry option strongly depends on the drilling cost for horizontal and vertical wells. We completed a bibliography study to establish and compare the cost of horizontal and vertical well perforation.

Finally, we performed a case study of CO<sub>2</sub> injection through various injections wells and evaluate the reservoir overpressure and the CO<sub>2</sub> storage cost.

Keywords	Horizontal vs. vertical wells, injection depth, overpressure from different wells, CO <sub>2</sub> storage costs.
----------	-------------------------------------------------------------------------------------------------------------------



## Table of Contents

<b>1. Introduction .....</b>	<b>3</b>
<b>2. Effect of the penetration of the injection well on the CO<sub>2</sub> injection pressure evolution .....</b>	<b>3</b>
<b>3. Impact of CO<sub>2</sub> injection through horizontal and vertical wells on the caprock mechanical stability .....</b>	<b>8</b>
3.1 Introduction .....	8
3.2 Results .....	9
3.3 Discussion.....	16
3.4 Conclusions.....	16
<b>4. CO<sub>2</sub> storage cost study for different injection geometries.....</b>	<b>18</b>
4.1 Horizontal and vertical wells perforation.....	18
4.2 CO <sub>2</sub> storage costs.....	21
4.3 Case study .....	22
<b>5. References.....</b>	<b>30</b>

## 1. Introduction

The overall objective of WP5 is to define optimal injection strategies and modes of injection, to (i) maximize the trapping while (ii) minimizing the reservoir pressure build-up and (iii) minimizing the energy usage and other major costs of the operation.

This is achieved through the following secondary objectives:

- Plan and implement injection strategies, firstly for the experiments to be carried out within the frame of this project (WP2). This includes (i) testing of different modes of injection, (ii) evaluating the trade-offs of injecting dissolved CO<sub>2</sub>, (iii) assessing the effectiveness of different injection geometries and (iv) envisaging testing injection of CO<sub>2</sub> micro-bubbles in brine.
- Extend the analyses, by means of modeling, to other conditions and site characteristics.
- Analyze results and suggest recommendations on best practices for injection, from the outlet of the supply line to the reservoir and the related pressure management.

This deliverable addresses the effectiveness of different injection geometries.

To this end, different injection geometries (injection in several wells, horizontal wells, injection close to caprock or deeper in the formation) have been tested by means of model analyses. In particular, we have tested whether efficient use of the pore space can be optimized in large scale operations by sequential injection in several wells. Criteria of comparison used here are the injectivity, pressure build-up, effective usable storage capacity, as well as drilling and energy costs.

## 2. Effect of the penetration of the injection well on the CO<sub>2</sub> injection pressure evolution

We assume injection of CO<sub>2</sub> through a vertical well in a 200 m thick saline aquifer with an intrinsic permeability of  $10^{-13}$  m<sup>2</sup>. The top of the aquifer is placed at 1.5 km deep. The injection rate is of 1 Mt of CO<sub>2</sub> per year. We consider 4 cases, a fully penetrating well, and 3 cases in which the injection well does not arrive to the bottom of the saline aquifer, with injection thickness of 50, 100 and 150 m.

Figure 2.1 shows the injection pressure evolution at the top of the aquifer when the permeability of the aquifer is isotropic. The required overpressure to inject a constant mass flow rate of CO<sub>2</sub> becomes higher as the thickness of injection well decreases at the beginning of injection. This transient increase in overpressure occurs due to permeability reduction while the CO<sub>2</sub> plume develops. However, once CO<sub>2</sub> displaces the formation brine away from the injection well, CO<sub>2</sub> becomes the dominant phase and the permeability reduction caused by a low relative permeability vanishes. Furthermore, since CO<sub>2</sub> viscosity is around one order of magnitude lower than that of brine, CO<sub>2</sub> flows easily inside of the aquifer, which causes a slight decrease of injection pressure.

Interestingly, the long-term injection pressure, i.e., after the CO<sub>2</sub> plume has fully developed around the injection well, is very similar regardless of the thickness of the injection well. This is because CO<sub>2</sub> advances mainly through the top of the aquifer due to buoyancy (Figure 2.2).

A very small injection thickness, i.e., one fourth of the aquifer thickness, requires a slightly higher injection pressure, which for an injection of 30 or 50 years may result in a significant over cost. However, when injecting through half of the aquifer, the resulting injection pressure is practically the same as when injecting through the whole aquifer, so the excavation costs of the injection well can be lowered without adding an extra cost for the compression at the wellhead. Furthermore, the additional

overpressure at the beginning of injection can be avoided if the CO<sub>2</sub> mass flow rate is progressively increased until CO<sub>2</sub> fill the pores in the vicinity of the injection well.

### Injection pressure evolution at the top of the aquifer

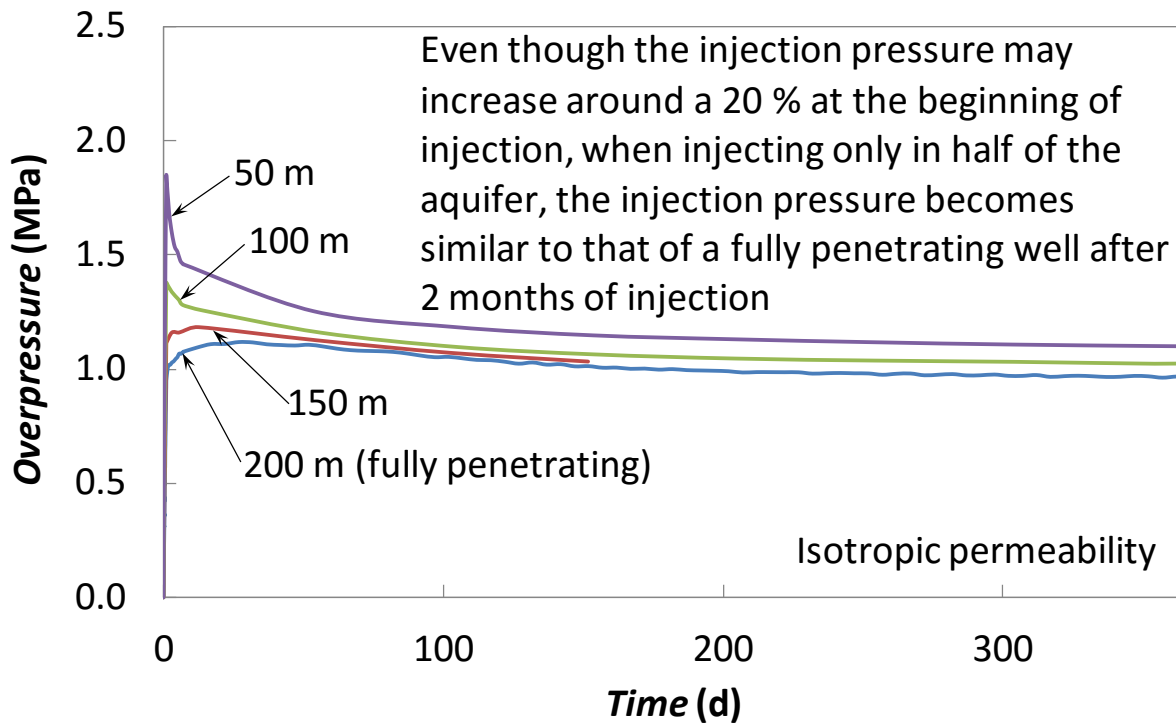


**Figure 2.1:** Injection pressure evolution as a function of the thickness of the injection well for a saline aquifer with an isotropic permeability of  $10^{-13} \text{ m}^2$ .

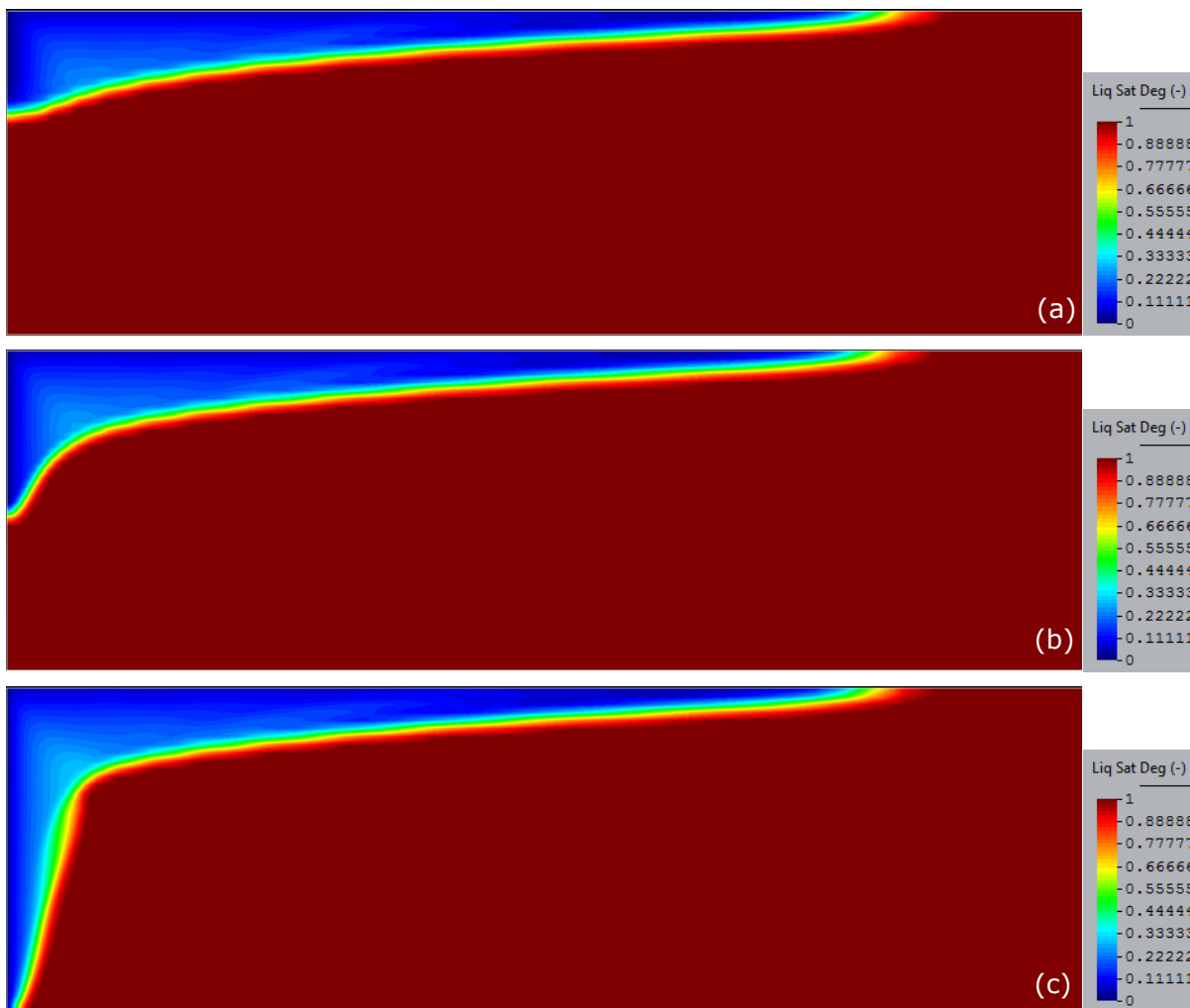


**Figure 2.2:** CO<sub>2</sub> plume shape after 1 year of injecting 1 Mt of CO<sub>2</sub> when injecting through (a) a well that penetrates only in the upper 50 m of a 200-m thick saline aquifer, (b) a well that penetrates only the upper half of the aquifer and (c) a well that fully penetrates the aquifer for the case of an aquifer with isotropic permeability of  $10^{-13}$  m<sup>2</sup>.

We perform the same analysis, but in an aquifer which vertical permeability is one order of magnitude lower than the horizontal permeability (Figure 2.3). Simulation results are similar to the case with isotropic permeability, but the initial differences in overpressure are larger because the lower vertical permeability delays the development of the CO<sub>2</sub> plume around the injection well and the CO<sub>2</sub> flow towards the top of the aquifer (Figure 2.4). Nevertheless, the slight over cost in compression energy when injecting through just the upper half of the aquifer may still offset the higher cost of drilling the injection well until the bottom of the saline aquifer.

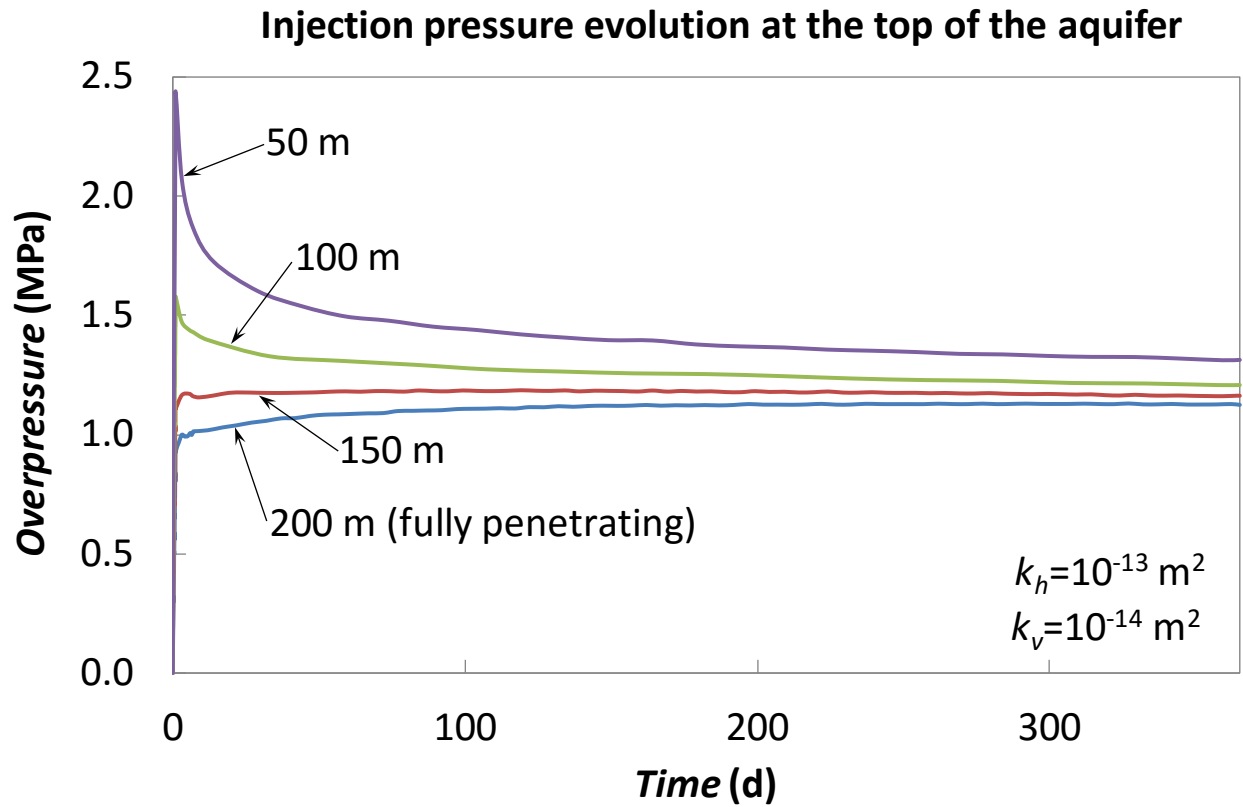


**Figure 2.3:** Injection pressure evolution as a function of the thickness of the injection well for a saline aquifer with a horizontal permeability of  $10^{-13} \text{ m}^2$  and a vertical permeability of  $10^{-14} \text{ m}^2$ .

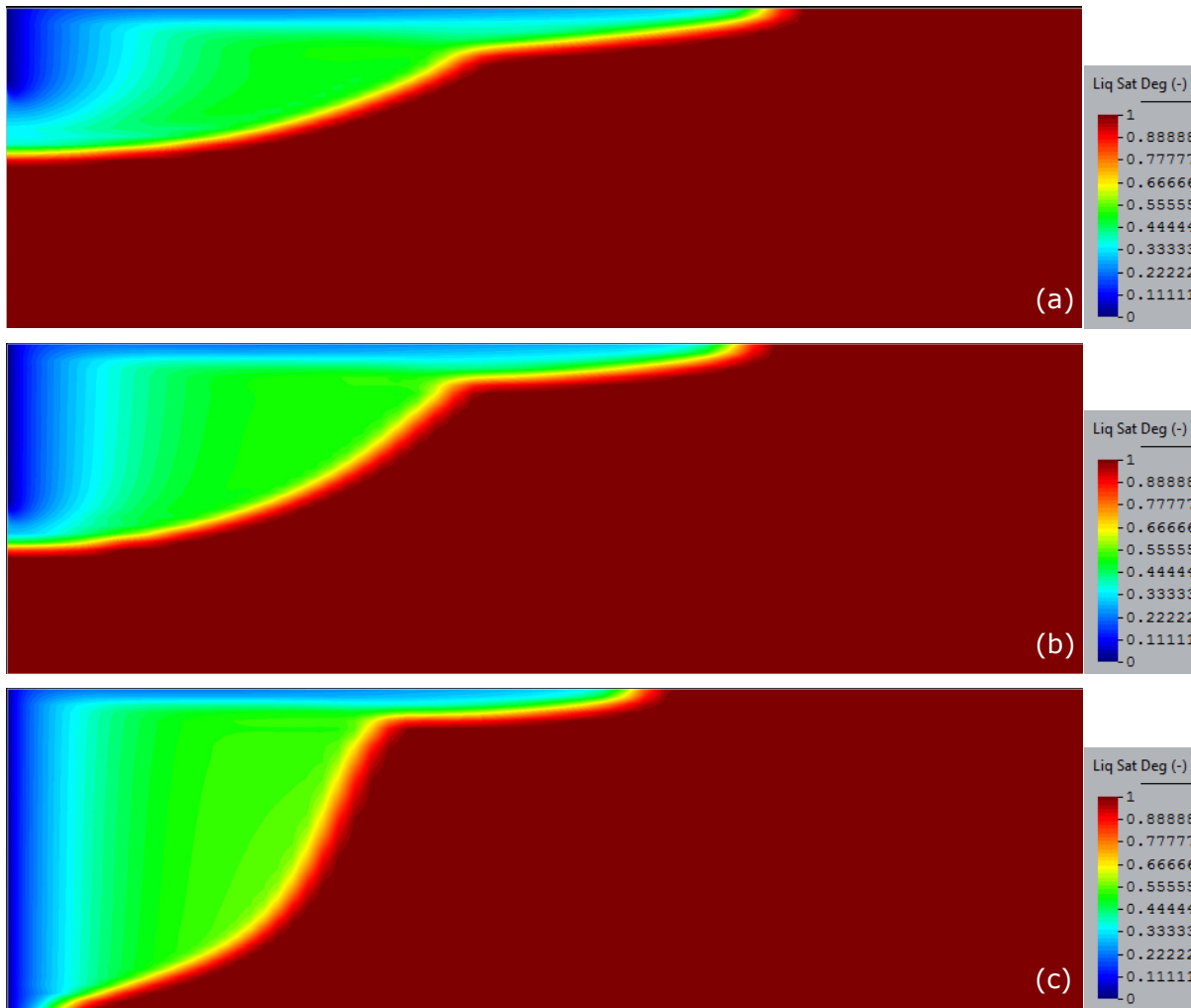


**Figure 2.4:** CO<sub>2</sub> plume shape after 1 year of injecting 1 Mt of CO<sub>2</sub> when injecting through (a) a well that penetrates only in the upper 50 m of a 200-m thick saline aquifer, (b) a well that penetrates only the upper half of the aquifer and (c) a well that fully penetrates the aquifer for the case of an aquifer with horizontal permeability of  $10^{-13}$  m<sup>2</sup> and a vertical permeability of  $10^{-14}$  m<sup>2</sup>.

## 3. Impact of CO<sub>2</sub> injection through horizontal and vertical wells on the caprock mechanical stability

### 3.1 Introduction

The large amounts of carbon dioxide (CO<sub>2</sub>) (of the order of 8 Gt/yr by 2050 [IEA, 2010]) that will be injected in deep saline formations are likely to generate large overpressures that may jeopardize the caprock mechanical stability [Rutqvist, 2012]. This overpressure may trigger induced microseismicity [Hsiesh and Bredehoeft, 1981; Soltanzadeh and Hawkes, 2009; Evans et al., 2012], which could lead to the open up of a leakage path for CO<sub>2</sub>. Even though no felt seismic event related to CO<sub>2</sub> injection has been recorded to date [Rutqvist, 2012], induced microseismic events have been measured by geophones placed at depth [Bohnhoff et al, 2010; Verdon et al, 2011]. As a result, coupled hydro-mechanical processes related to GCS are gaining importance and an increasing number of studies focus on this topic [Rutqvist et al, 2008; Ferronato et al, 2010; Vilarrasa et al, 2010; Goerke et al, 2011; Alonso et al, 2012].

The hydro-mechanical response of the reservoir and caprock is strongly related to fluid pressure evolution, which is controlled by the orientation of the CO<sub>2</sub> injection well, i.e. vertical or horizontal well (Figure 3.1). CO<sub>2</sub> pressure evolution in a vertical well has been studied analytically in laterally extensive saline aquifers [Mathias et al, 2009; Vilarrasa et al, 2010] and in closed saline aquifers, i.e. surrounded by a low-permeability boundary [Zhou et al, 2008, Mathias et al, 2011a, Mathias et al, 2011b]. The effect of a low-permeability boundary is an increase of overpressure in the whole saline aquifer, which may cause caprock mechanical instability. This increase in overpressure starts once the fluid pressure perturbation front reaches the low-permeability boundary. When injecting CO<sub>2</sub> at a constant mass flow rate through a vertical well, injection pressure increases sharply at the beginning of injection both because the viscosity of the displaced brine is high and because the relative permeability to CO<sub>2</sub> is low before CO<sub>2</sub> establishes connected flow paths within the pore network and is able to flow readily.

However, injection pressure slowly decreases once CO<sub>2</sub> fills the pores in the vicinity of the injection well and the capillary fringe is displaced away from the injection well because (i) the relative permeability to CO<sub>2</sub> increases around the well, (ii) the pressure drop across the capillary fringe is reduced (it is inversely proportional to the radius of the capillary fringe) and (iii) the viscosity of CO<sub>2</sub> is much lower than that of the brine (around one order of magnitude).

As a result, mechanical stability tends to improve with time. By contrast, the injection of a constant CO<sub>2</sub> mass flow rate through a horizontal well induces a continuous increase of fluid pressure with time [Zhang and Agarwal, 2012; Rutqvist and Tsang, 2002]. This is mainly because relative permeability to CO<sub>2</sub> remains low between the injection well, which is usually placed at the bottom of the saline aquifer, and the top of the saline aquifer, where CO<sub>2</sub> accumulates and spreads laterally.

Therefore, CO<sub>2</sub> cannot flow easily through well-connected paths, inducing a progressive buildup of injection pressure. This continuous increase in fluid pressure may yield failure conditions after several years of injection.

Given this significant difference between the fluid pressure evolution of vertical and horizontal wells, one may conjecture that CO<sub>2</sub> injection through vertical wells may be mechanically more favorable than through horizontal wells, at least for injection timescales of several decades. However, the stress field is usually modified as a result of fluid pressure changes [Streit and Hillis, 2004]. Therefore, we perform fully coupled hydro-mechanical simulations to analyze the suitability of CO<sub>2</sub> injection through horizontal

and vertical wells and to determine whether the caprock mechanical stability could be damaged (Vilarrasa, 2014).

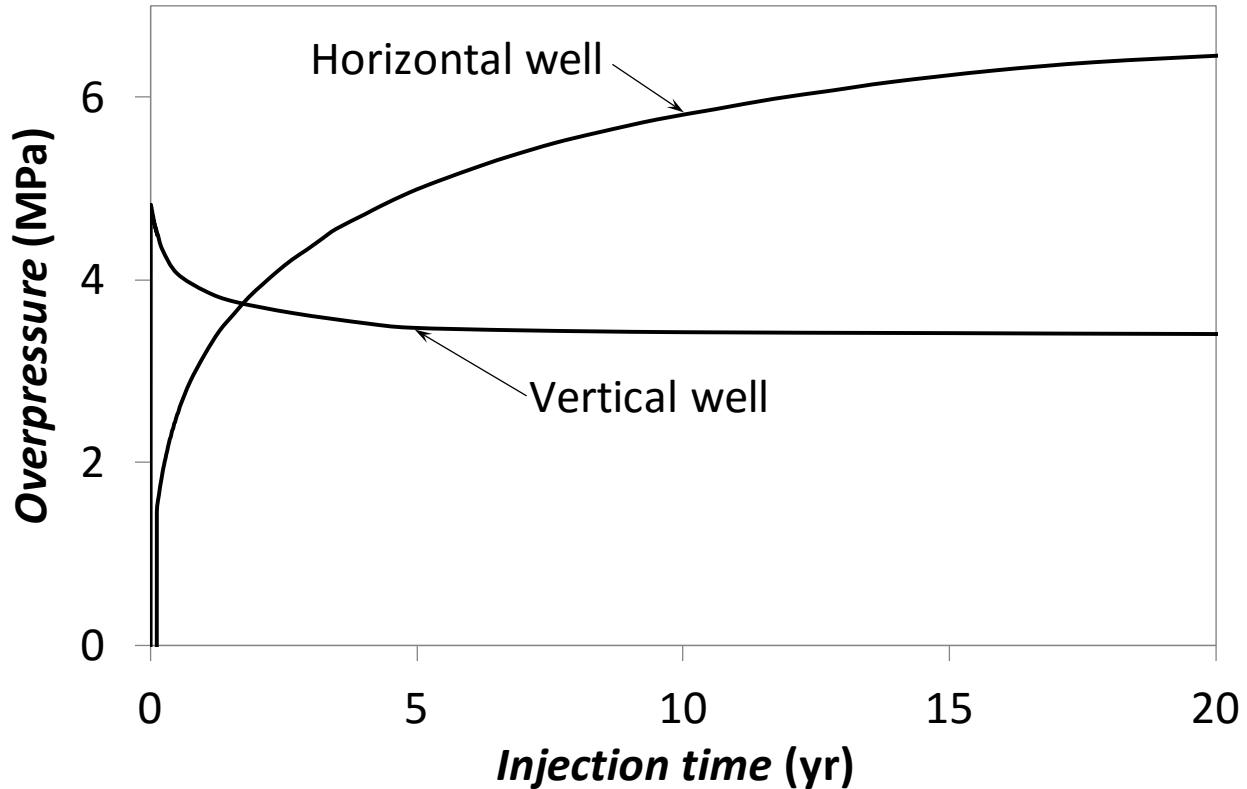


**Figure 3.1:** Overpressure evolution at the top of the aquifer next to the injection well casing when injecting CO<sub>2</sub> through a vertical and a horizontal well at a constant mass flow rate.

## 3.2 Results

Since fluid pressure evolution is significantly different when injecting CO<sub>2</sub> through a vertical well than through a horizontal well, the induced changes in the effective stress field differ as well. This is reflected in a plot that shows the deviatoric stress versus the mean effective stress ( $q - \sigma'_m$ ) trajectories (Figures 3.2 and 3.3).

When injecting a constant mass flow rate of CO<sub>2</sub> through a vertical well, the sharp increase in fluid pressure at the beginning of injection produces, in the saline aquifer, a rapid decrease in the mean effective stress, while the deviatoric stress remains nearly constant (Figure 3.2a and 3.3a). Thus, the stress state approaches failure conditions at the beginning of injection.

However, once CO<sub>2</sub> pressure drops, the mean effective stress increases, leading to a safer situation. Additionally, horizontal total stresses increase as a response to fluid pressure buildup [Ruqvist 2012, Streit and Hillis, 2004, de Simone et al, 2013]. This causes the deviatoric stress to decrease in a NF stress regime (because the horizontal stress is the minimum and since it increases, the Mohr circle becomes smaller) and to increase in a RF stress regime (because the horizontal stress is the maximum and since it increases, the Mohr circle becomes bigger).

Fluid pressure evolution in the caprock is somewhat different because of mechanical effects that lead to a pressure drop at the beginning of injection rather than an increase, which is known as the Noordbergum effect [Barton et al, 1985, Yeo et al, 1998]. This leads to an improvement of the caprock mechanical stability at the beginning of injection that is followed by a small decrease in stability once overpressure propagates across the low-permeability caprock, which can last several days or weeks (Figure 3.2b and 3.3b). This decrease in caprock stability is more pronounced in a RF stress regime than in a NF stress regime because in a RF stress regime the deviatoric stress increases as the horizontal total stresses increase.

On the other hand, CO<sub>2</sub> pressure builds up progressively when injecting CO<sub>2</sub> through a horizontal well. This results in a simultaneous reduction in the mean effective stress and deviatoric stress that yields a  $q - \sigma'_m$  trajectory that is almost parallel to the failure envelope in a NF stress regime (Figure 3.2a). Similarly, the trajectory in the caprock is quite parallel to the failure envelope (except for some abrupt changes in the trajectory direction that are due to CO<sub>2</sub> breaking through into the caprock and will be explained in detail later). So despite the continuous CO<sub>2</sub> pressure buildup, failure conditions are unlikely to occur in this particular scenario (Figure 3.2b). However, in a RF stress regime the deviatoric stress in the saline aquifer increases rather than decreases as fluid pressure builds up (Figure 3.3a). This trend also occurs in the caprock (Figure 3.3b), which presents some abrupt changes in the trajectory direction that are due to CO<sub>2</sub> breaking through into the caprock.

These results may be surprising because, while it is clear that the mean effective stress decreases when fluid pressure increases, it may not be obvious why the deviatoric stress should change.

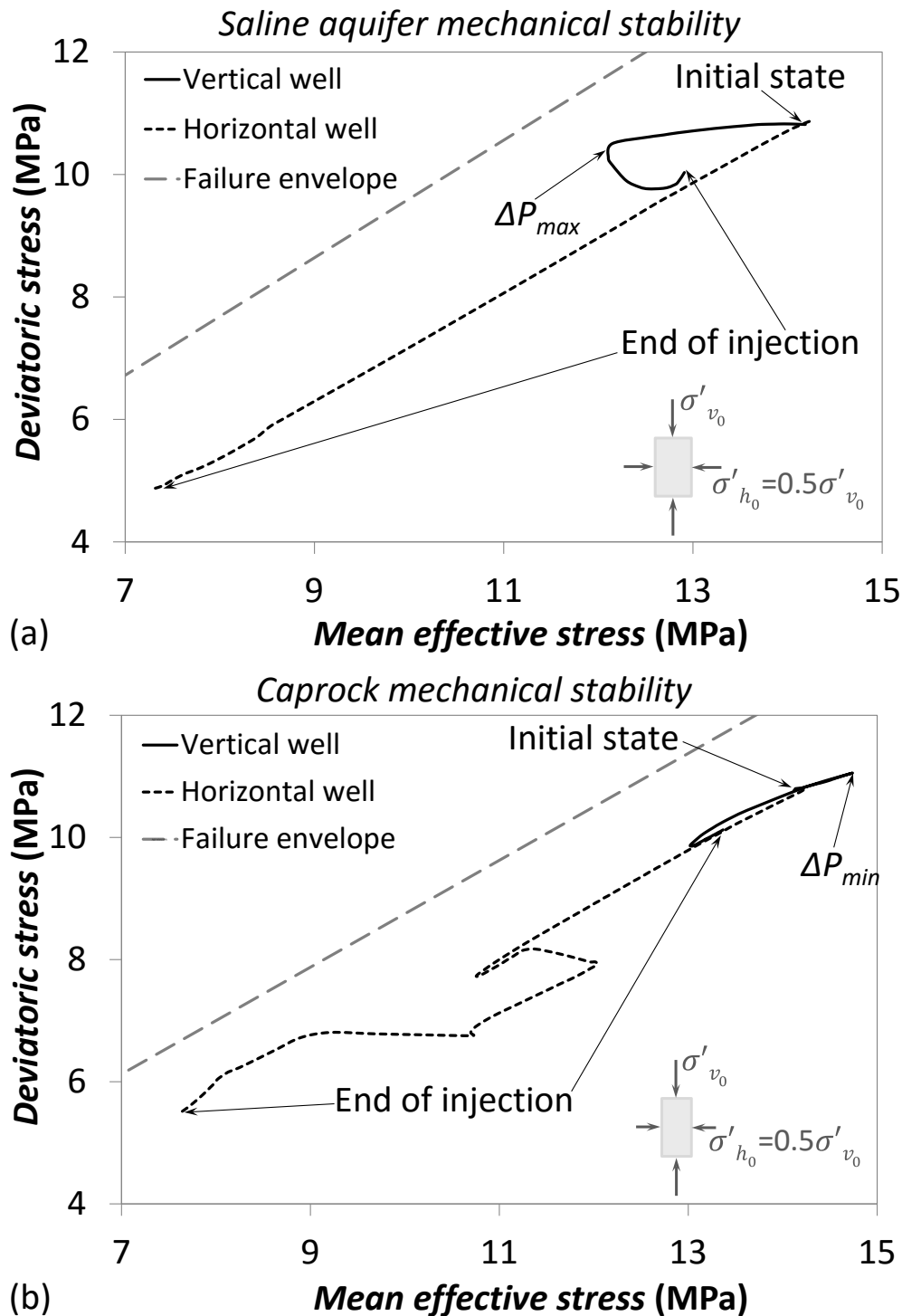


**Figure 3.2:**  $q - \sigma'_m$  trajectories for a vertical and a horizontal well in a normal faulting stress regime (a) at the top of the saline aquifer next to the injection well casing and (b) at a point of the caprock placed 5 m above the saline aquifer next to the injection well casing.

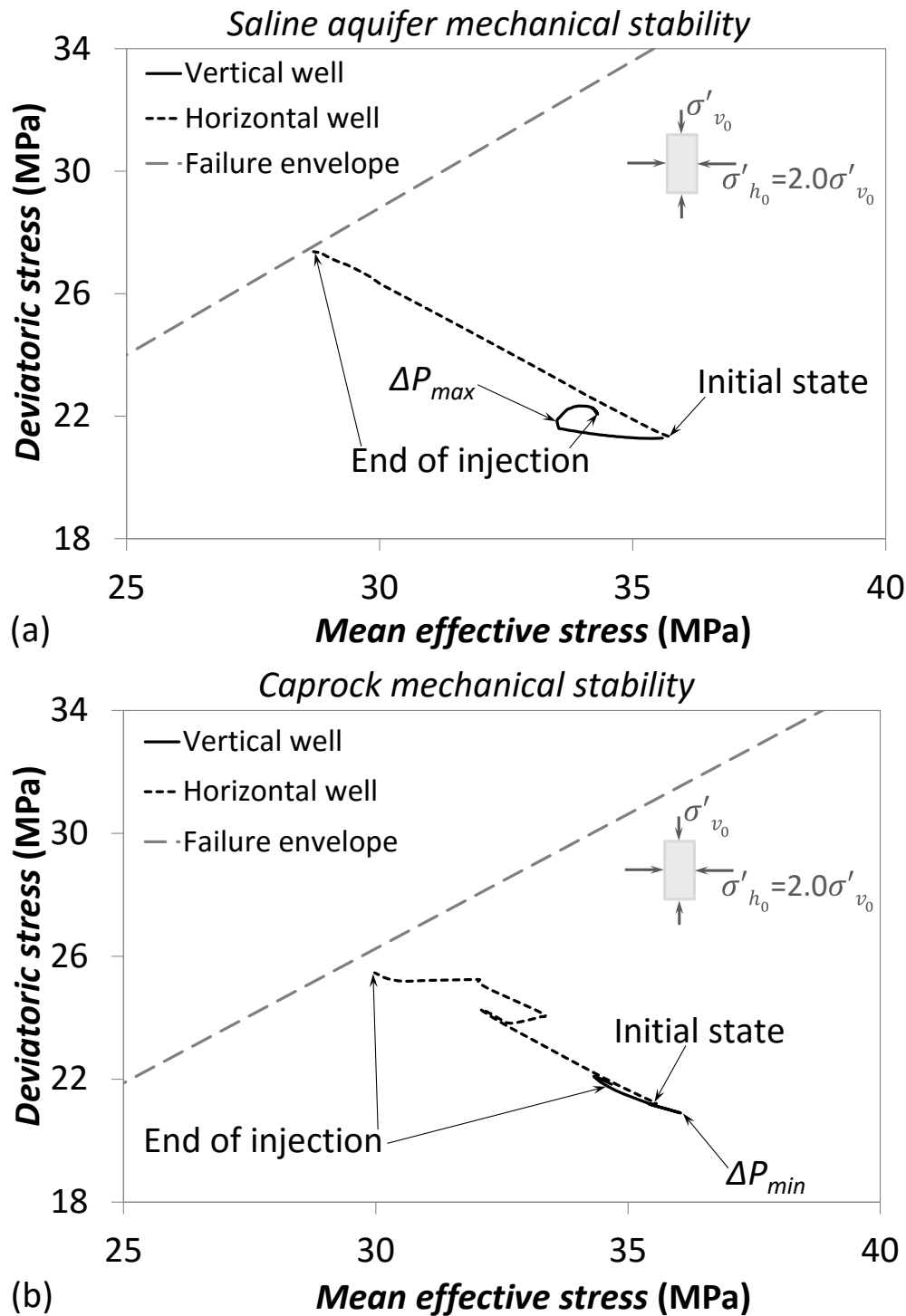


**Figure 3.3:**  $q - \sigma'_m$  trajectories for a vertical and a horizontal well in a reverse faulting stress regime (a) at the top of the saline aquifer next to the injection well casing and (b) at a point of the caprock placed 5 m above the saline aquifer next to the injection well casing.

Figures 3.4 and 3.5 show the overpressure, the deviatoric and the mean effective stress evolution in a point of the caprock that is placed next to the well casing and 5 m above the saline aquifer. This point is representative of the lower region of the caprock, which is the most critical because of its proximity to the saline aquifer. When injecting through a vertical well (Figures 3.4a and 3.5a), fluid pressure drops at the beginning of injection (for a few days) because of the deformation induced by injection, which produces an expansion of the pore volume within the caprock. This leads to an improvement of the caprock mechanical stability at the beginning of injection, which is followed by a worsening as fluid pressure perturbation propagates through the low-permeability caprock. Nevertheless, the changes are small in the scenarios considered in this study, so the caprock mechanical stability is unlikely to be compromised unless the rock is critically stressed.

For a horizontal well (Figure 3.4b and 3.5b), the caprock mechanical stability presents some abrupt changes in stability, which are related to CO<sub>2</sub> breaking through into the caprock. CO<sub>2</sub> penetrates into the caprock in this particular case because of the high overpressure, which leads to a capillary pressure higher than the caprock entry pressure. Initially, the induced overpressure in the saline aquifer propagates into the lower part of the caprock, but with a lower magnitude. Therefore, horizontal stresses increase in the caprock, causing an improvement in caprock stability in a NF stress regime (because the deviatoric stress decreases) and a worsening in a RF stress regime (because the deviatoric stress increases). When CO<sub>2</sub> first penetrates into the caprock (after 6 yr of injection), it causes an increase of the horizontal total stresses, which tightens the lower part of the caprock, where CO<sub>2</sub> has not arrived yet. This specially affects a caprock in a NF stress regime, improving the caprock mechanical stability (Figure 3.4b).

However, this effect is much smaller in a RF stress regime, because the confining stress is already large (Figure 3.5b). But once CO<sub>2</sub> reaches the observation point (after 12 yr), fluid pressure increases sharply, which produces a decrease of effective stresses. Thus, stability is worsened significantly, which could contribute to an enhancement of CO<sub>2</sub> flux through the caprock if it were to yield.

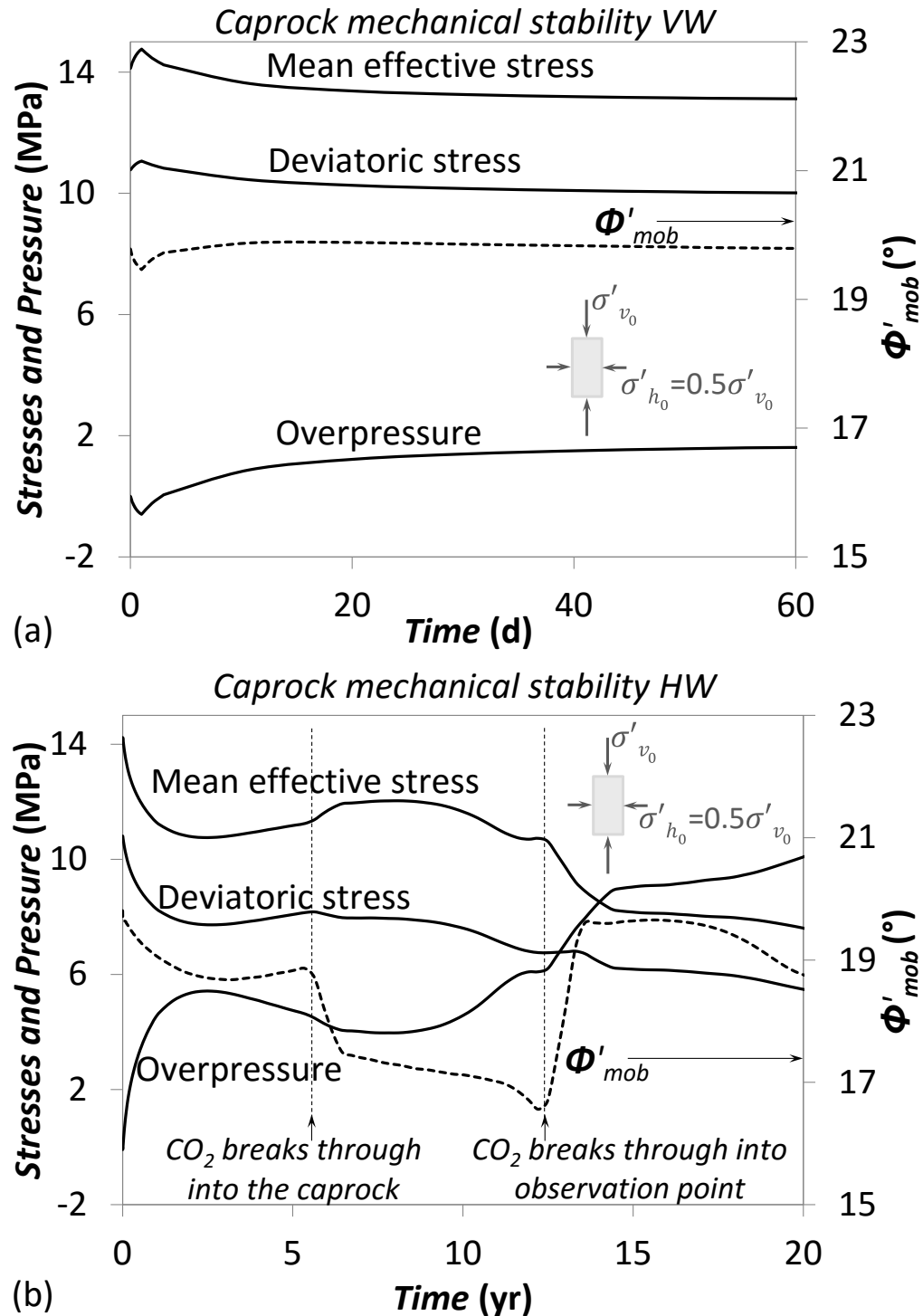


**Figure 3.4:** Stress, overpressure and mobilized friction angle evolution in a normal faulting stress regime at a point of the caprock placed 5 m above the saline aquifer next to the injection well casing (a) for a vertical well (VW) and (b) for a horizontal well (HW).

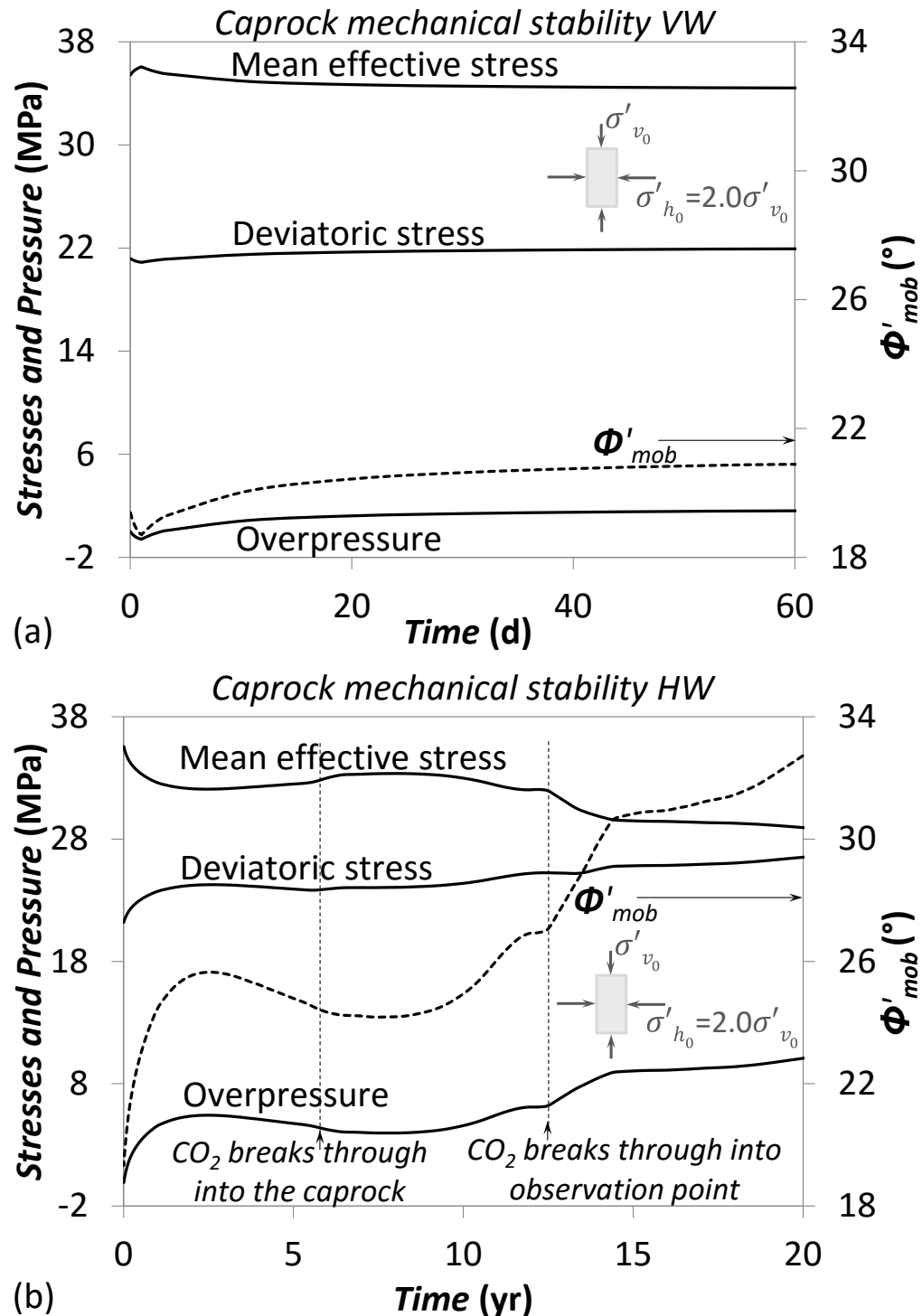


**Figure 3.5:** Stress, overpressure and mobilized friction angle evolution in a reverse faulting stress regime at a point of the caprock placed 5 m above the saline aquifer next to the injection well casing (a) for a vertical well (VW) and (b) for a horizontal well (HW).

## 3.3 Discussion

The conjecture that the rock mechanical stability would be more favorable for CO<sub>2</sub> injection through vertical than horizontal wells for long injection times (decades) is not necessarily valid. This is because even though fluid pressure increases continuously when injecting through a horizontal well, horizontal total stresses also increase, leading to a reduction of the deviatoric stress for a NF stress regime. However, this increase in the horizontal total stresses enlarges the deviatoric stress in a RF stress regime, leading to unstable conditions both in the saline aquifer and the caprock. Therefore, microseismic events are likely to occur, which could open up leakage paths.

On the other hand, the most critical situation in the saline aquifer occurs at the beginning of injection through a vertical well, coinciding with the peak in overpressure. To minimize the risk of inducing microseismicity, CO<sub>2</sub> injection rate can be progressively increased at the beginning, so that fluid pressure builds up more gradually. However, induced microseismic events are not necessarily negative if they are triggered within the saline aquifer because microseismicity is related to shear slip, which increases permeability of rough fractures, especially in the direction perpendicular to shear [Barton et al, 1985; Yeo et al, 1998; Vilarrasa et al, 2011]. Therefore, injectivity would be enhanced and a lower overpressure would be necessary for injecting the same amount of CO<sub>2</sub>.

Here, we have considered a saline aquifer of extensive lateral dimensions. However, heterogeneity, such as faults, may exist relatively close to the injection well. If a fault behaves as a flow barrier, overpressure will increase, which eventually could trigger induced seismicity. Undetected flow barriers can pose a risk to rock mechanical stability if fluid pressure increases significantly. Therefore, monitoring injection pressure evolution is crucial to guarantee that induced seismicity that could be felt by local population will not be triggered and that no leakage path is created. Deviations from the expected fluid pressure evolution should be analyzed and mitigation measures should be carried out if overpressure increases unexpectedly.

## 3.4 Conclusions

CO<sub>2</sub> pressure evolution is significantly different when injecting a constant CO<sub>2</sub> mass flow rate through a vertical or a horizontal well. Fluid pressure near the injection well increases sharply at the beginning of injection (for a few days) through a vertical well, but afterwards it drops slightly. Therefore, the rock mechanical stability is reduced in the saline aquifer at the beginning of injection, but it improves after the initial peak in fluid pressure. Nevertheless, the induced changes are small in the cases considered in this study. By contrast, fluid pressure continuously builds up when injecting through a horizontal well and for a common length of horizontal wells (around 2 km) the induced overpressure is larger than that of a vertical well. Not only does overpressure produce a gradual reduction in the mean effective stress, but also an increase of the horizontal total stresses because of the lateral confinement. When overpressure is significantly high (of the order of 10 MPa), the increase of horizontal total stresses leads to a more stable situation in the NF stress regime considered in this study (the deviatoric stress decreases), but could lead to unstable conditions in a RF stress regime (the deviatoric stress increases). This high overpressure gives rise to a capillary pressure that exceeds the caprock entry pressure, so CO<sub>2</sub> penetrates through the lower portion of the caprock. However, overpressure becomes comparable of that induced by a vertical well in the presence of a caprock with a relatively high permeability or a longer injection well. In these cases, neither the reservoir nor the caprock mechanical stability is likely to be compromised because the effective stress changes induce relatively small changes in the mobilized friction angle. Thus, CO<sub>2</sub> injection at a constant mass flow rate through a vertical well is



# TRUST



unlikely to yield unstable conditions both in NF and RF stress regimes in extensive saline aquifers like the one considered in this study. However, when injecting through a horizontal well the increase in horizontal total stresses improves the reservoir and caprock mechanical stability in a NF stress regime, but worsens it in a RF stress regime when a high overpressure is induced. These changes in the stress field highlight the importance of solving coupled hydro-mechanical simulations to assess the rock mechanical stability of geologic carbon storage projects.

## 4. CO<sub>2</sub> storage cost study for different injection geometries

### 4.1 Horizontal and vertical wells perforation

The average horizontal well is more expensive and technically difficult to drill than the average vertical well. Yet, around the world, horizontal wells are being spudded in ever increasing numbers. Almost 80% of the wells being drilled in Oman, Qatar and Abu Dhabi are horizontal. Why should this be? In simple terms, horizontal wells allow us to do things more efficiently than vertical wells. It would be short-sighted to ignore a technique which offers improved drainage in typical reservoirs and penetrates more of the discrete compartments in complex reservoirs, while helping to reduce gas and water coning. Throughout the Middle East, horizontal wells are being used for field developments which, in the past, would have relied on vertical wells. While the basic geology of many Middle East fields is well known, details of reservoir structure, faulting, facies and pore system heterogeneity are not usually so well-defined.

The recent increase in horizontal drilling has helped reservoir engineers and geoscientists to understand the lateral variations, permeability barriers and compartments which occur between existing vertical wells. Using horizontal wells we can locate leached zones, find unconformities and probe pinchouts and other sites with by-passed oil potential.

Horizontal wells are usually drilled to enhance oil production. In some situations the improvement may be dramatic - enabling development of a reservoir which would otherwise have been considered marginal or uneconomic.

However, in cases where the improvement is likely to be less spectacular, horizontal drilling costs and benefits must be assessed carefully.

There are many kinds of reservoir where the potential benefits of horizontal drilling are obvious.

- Thin reservoirs: a vertical well drilled into a thin reservoir will have a very small contact surface (effectively limited by reservoir thickness) with the oil-producing horizon. A horizontal well in the same reservoir layer can have a contact surface running the length of the reservoir.
- Reservoirs with natural vertical fractures: horizontal wells typically intersect thousands of small vertical fractures and, if the reservoir contains them, some very large ones. If the well trajectory has been planned carefully these large vertical fractures can be used to improve productivity, even when the overall fracture density is low. However, if a fault fracture system is misinterpreted the result may be early water or unwanted gas production. The damage which an inappropriate horizontal well can cause underlines the importance of having a good reservoir model before drilling begins or being able to assess the well accurately during or after drilling.
- Reservoirs where water (and gas) coning will develop: the flow geometry associated with a horizontal drain helps to reduce the amount of water or gas coning in any given reservoir.
- This means that the total volume of oil recovered before water or gas break-through can be increased. The only potential obstacle to a significant increase in oil recovery rate is the presence of zones with high vertical permeability (e.g. the faults and fault-related fractures

mentioned above). However, with advance planning, these can be dealt with using selective completion techniques.

- Horizontal wells remove oil from a reservoir over a long producing zone at relatively slow rates. In contrast, vertical wells take oil very quickly through much shorter lengths of borehole. The flow geometry associated with horizontal wells tends to reduce the influence of heterogeneity along the long drain – so increasing total production.
- Thin layered reservoirs: oil recovery from water flooding can be improved dramatically by injecting and producing from horizontal wells, rather than using vertical wells in a traditional water flood.
- Heterogeneous reservoirs: horizontal heterogeneity in reservoirs presents a problem for vertical wells - they can only access those reservoir compartments which lie immediately below the drilling rig. Horizontal wells can be used to search for isolated and by-passed oil and gas accumulations within a field

Horizontal wells cost more than vertical wells - so what do they offer in return? In problematic wells, for example, where there is a thin oil column or a risk of early water or gas production, vertical wells are usually very inefficient. A comparison of horizontal and vertical well performance (figure 4.1) clearly illustrates the potential benefits. Every horizontal well in this example gives better results than its vertical counterpart. Higher oil rates, coupled with greatly reduced gas-oil ratios, have made horizontal wells the first choice for many reservoirs. In some countries, such as Qatar, Abu Dhabi and Oman, horizontal drilling has become standard practice, with the vertical drilling alternative being examined on a well-by-well basis.

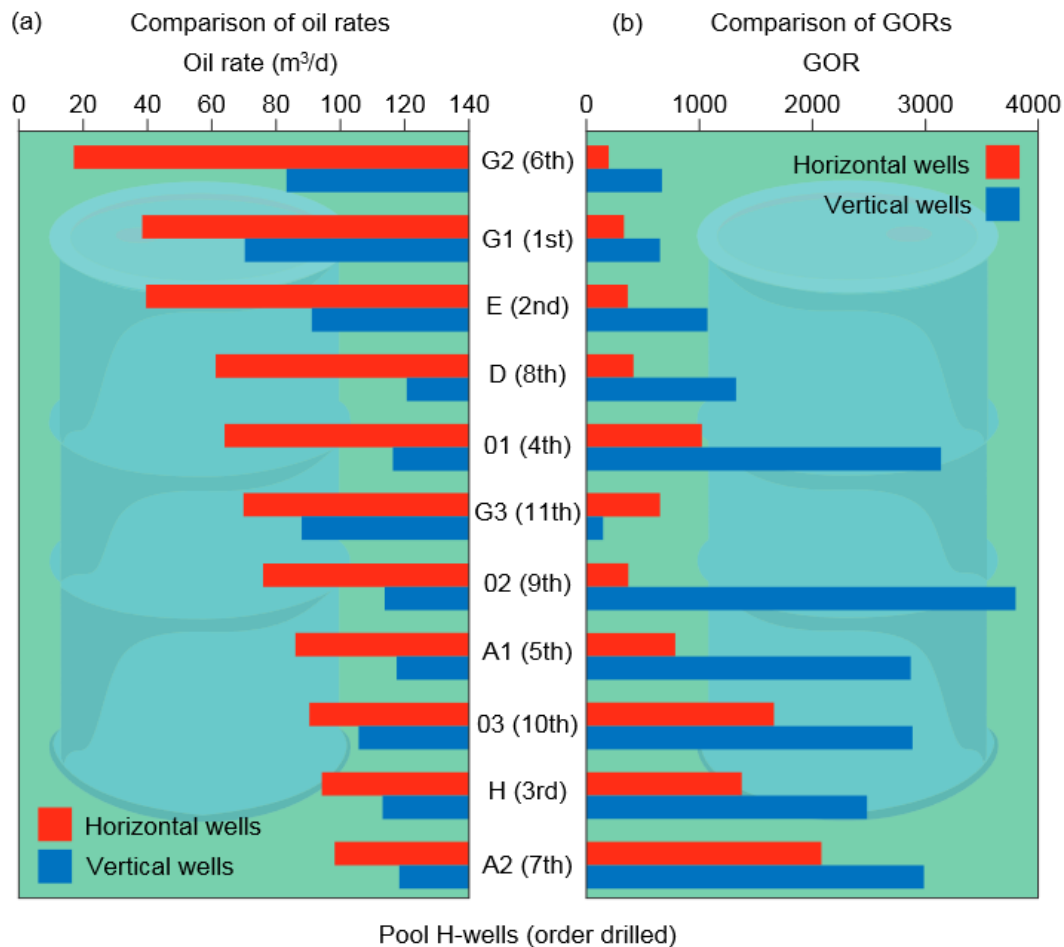


**Figure 4.1:** BALANCE SHEET: Horizontal wells produce higher volumes of oil (a) and smaller amounts of gas (b) than equivalent vertical wells. This sequence of wells is arranged in order of decreasing oil rate production for horizontal wells. This example is from Canada’s Devonian Rainbow Reef Reservoir, where lateral entry allowed the operator to produce oil without a high proportion of gas. Modified from F.J. McIntyre, et al. (1994).

In the U.S., the majority of applications are in low permeability, naturally fractured, carbonate reservoirs. However, in California, Alaska and Gulf of Mexico most of the wells are drilled in clastic reservoirs. Similarly, outside the U.S., most of the horizontal wells are drilled in clastic reservoirs. Horizontal wells have been used to produce thin zones, fractured reservoirs, formations with water and gas coning problems, waterflooding, heavy oil reservoirs, gas reservoirs, and in EOR methods such as thermal and CO<sub>2</sub> flooding.

## Cost/Benefits of Horizontal Wells

Disadvantages of horizontal wells are:

1. High cost as compared to a vertical well. In the U.S., a new horizontal well drilled from the surface, costs 1.5 to 2.5 times more than a vertical well. A re-entry horizontal well costs about 0.4 to 1.3 times a vertical well cost.
2. Generally only one zone at a time can be produced using a horizontal well. If the reservoir has multiple pay-zones, especially with large differences in vertical depth, or large differences in permeabilities, it is not easy to drain all the layers using a single horizontal well.
3. The overall current commercial success rate of horizontal wells in the U.S. appears to be 65%. (This success ratio improves as more horizontal wells are drilled in the given formation in a particular area.) This means, initially it is probable that only 2 out of 3 drilled wells will be commercially successful. This creates extra initial risk for the project.

Benefits of horizontal wells are:

1. Higher rates and reserves as compared to vertical wells. This result in less finding cost and less operating cost per barrel of oil produced. In the U.S., in places where vertical well operating costs are \$7 to \$9 per barrel of oil, the horizontal well operating costs are \$3 to \$4 per barrel.
2. For many horizontal well projects, the finding (developing) cost, defined as well cost divided by well reserves, is about \$3 to \$4/bbl. This is about 25% to 50% lower than the cost of buying proved producing reserves.
3. To produce the same amount of oil, one needs fewer horizontal wells as compared to vertical wells. This results in reduced need for surface pipelines, locations, etc.

Same benefits can be applied for CO<sub>2</sub> storage (section 3).

## 4.2 CO<sub>2</sub> storage costs

Costs for geologic storage are highly variable because of the heterogeneity of storage reservoirs. This includes reservoir type (e.g., onshore vs. offshore, depleted field vs. deep saline formation) and reservoir geology (e.g., porosity, permeability, depth). Therefore the literature presents the cost of storage as a range. This range is based on the judgment of study authors rather than a detailed statistical analysis, in part because data on a large percentage of potential storage reservoirs is quite sparse. Poor candidates for storage reservoirs could have storage costs well above the high value of the reported ranges.

In the SRCCS the reported costs for CO<sub>2</sub> storage in geologic formations ranged from 0.5 to 8.0 2002 USD/tCO<sub>2</sub> with an additional cost for monitoring of 0.1–0.3 2002 USD/tCO<sub>2</sub>. More recently, ZEP (2011) reported costs as shown in Table 12 in 2010 EUR/tCO<sub>2</sub>. They broke down costs into onshore and offshore storage and separated saline formations from depleted oil and gas fields. Furthermore, for depleted fields, they looked at cases where existing infrastructure could or could not be reused.

The USDOE also recently developed a CO<sub>2</sub> Saline Storage Cost Model (USDOE, 2014). Using the model, they generated a cost-supply curve for the US. The graph has two inflection points, with over 70% of the storage capacity contained between these two points. Using these points as high/low estimates, the cost range is 7–13 2011 USD/tCO<sub>2</sub>.

The GCCSI (2011) reported storage costs for poor and good reservoir properties. Using these as low and high estimates, the range is 6–13 2010 USD/tCO<sub>2</sub>.

For EOR credits, the SRCCS reported a range of 10–16 2002 USD/tCO<sub>2</sub>. With sustained higher oil prices over the past decade—on the order of \$100/bbl—the demand for CO<sub>2</sub> has increased significantly for EOR (Suresh, 2010). This has led to potentially higher selling prices for CO<sub>2</sub>. Although the details of such transactions remain proprietary and are not publicly available, “conventional wisdom” suggests that the price that EOR projects can afford to pay for CO<sub>2</sub> (in \$/mcf, thousand standard cubic feet) is 2% of the oil price in \$/bbl. Therefore, oil at \$100/bbl translates into a CO<sub>2</sub> price of \$36/tCO<sub>2</sub> (Carbon Management Workshop, 2011).

Given the more recent drop in oil prices in 2014, as well as its historic volatility, Rubin et al. (2015) suggest a range of \$15–40/tCO<sub>2</sub> as the net credit (negative storage cost on a levelized basis) for CO<sub>2</sub> sold for EOR. Implicit in this range is the assumption that CO<sub>2</sub>-EOR will comply with future regulatory requirements for geological storage of CO<sub>2</sub>, which are still under development. To the extent that meeting future requirements incurs significant additional costs, the range suggested above may have to be modified.

As mentioned before, the cost of storage in geological subsurface varies according to site-specific factors such as onshore vs. offshore, reservoir depth, and geological characteristics. Costs associated with CO<sub>2</sub> storage have been estimated to be approximately \$0.4–20/tonne without EOR. Representative cost estimates in saline formations and depleted oil and gas reservoirs are between \$0.4–\$12 per tonne of CO<sub>2</sub> injected, with an additional \$0.16–\$0.30 per tonne for monitoring and verification (IPCC, 2005). Offshore costs tend to be on the upper end of these ranges. When CO<sub>2</sub> storage is combined with EOR or CBM, the economic value of CO<sub>2</sub> can result in a net benefit for injecting CO<sub>2</sub> underground (IPCC, 2005) as mentioned before.

## 4.3 Case study

In this section we propose a case study of CO<sub>2</sub> injection through several vertical injection wells. We calculate the pressure built-up due to the high CO<sub>2</sub> injection rate and the pressure transmission to the different wells. We then evaluate the CO<sub>2</sub> storage cost using the FE/NETL CO<sub>2</sub> Saline Storage Cost Model (Open Source Software License for Excel Spreadsheet) developed by National Energy Technology Laboratory (NETL), Tim Grant (DOE/National Energy Technology Laboratory), David Morgan (DOE/National Energy Technology Laboratory Energy Sector Planning and Analysis (ESPA)), Andrea Poe and Jason Valenstein (Booz Allen Hamilton, Inc.).

One of the most important issues when several wells are used to inject CO<sub>2</sub> into a target aquifer is the overpressure in one of them that their interaction may provoke. This overpressure obviously produces physical effects, but it also has an impact in the operational cost of the CO<sub>2</sub> sequestration. This latter aspect is the one that we focus on in this study.

In order to be able to calculate the overpressure generated in a well by a multiple injection scenario, we divide this overpressure calculation in two terms (Eq.4.1): the first one is the overpressure induced in the well by its own injection, and the second is the effect provoked in this well by the injection in other wells.

$$\Delta P_{i \text{ final}} = \Delta P_i + \sum_{j=1}^n \Delta P_{i \rightarrow j} \quad (4.1)$$

To estimate the first term, two analytical solutions have been proposed: the Nordbotten et al. (2005) solution and the Dentz and Tartakovsky (2009a) solution taking into account the CO<sub>2</sub> compressibility correction (Vilarrasa et al. 2010). Moreover, the position of the interface between the CO<sub>2</sub> rich phase and the formation brine is also calculated with these solutions.

The second term, namely the overpressure due to the interference with other injection wells, is calculated by assuming a single phase approach. In fact, the variation of pressure generated at great distance from the injection well can be estimated by solely taking into account the presence of the brine phase. Therefore, the overpressure at the well 'i' due to the injection into a well 'j' placed at distance *r* is easily calculated by means of the Theis solution (1935):

$$\Delta p(r) = \frac{Q_v}{4\pi k b} W(u) \quad [MPa] \quad (4.2)$$

Where  $Q_v$  is the volumetric injection rate of CO<sub>2</sub> (m<sup>3</sup>/s), *k* is the intrinsic permeability of the aquifer (m<sup>2</sup>), *b* is the aquifer thickness (m),  $\mu$  is the brine viscosity (Pa s),  $W(u)$  represents the well function and  $u = r^2 S_s \mu / (4kt)$  (being *t* the time and *S<sub>s</sub>* the storage term).

In this study we simulate four different scenarios of CO<sub>2</sub> injection into a saline aquifer. The parameters considered are listed in Table 4.1 and we suppose that three wells are being used to inject the same mass flow rate of CO<sub>2</sub> as specified in Table 4.1.

	t (yr)	Q <sub>m</sub> (Kg/s)	k (m <sup>2</sup> )	Φ (-)	Depth (m)	b (m)	ρ <sub>w</sub> (Kg/m <sup>3</sup> )	ρ <sub>c</sub> (Kg/m <sup>3</sup> )	r <sub>c</sub> (m)	N <sub>g</sub>
<b>Scenario 1</b>	30	41.22	10 <sup>-13</sup>	0.15	1000	100	1030	586.02	1	0.246
<b>Scenario 2</b>	30	41.22	10 <sup>-13</sup>	0.20	1000	100	1030	586.02	1	0.246
<b>Scenario 3</b>	30	41.22	5·10 <sup>-13</sup>	0.15	1000	100	1030	586.02	1	1.232
<b>Scenario 4</b>	30	41.22	5·10 <sup>-13</sup>	0.20	1000	100	1030	586.02	1	1.232

**Table 4.1:** Parameters considered for the simulations in the four injection scenarios.

The first part of the calculation is the overpressure generated in a well 'i' by its own injection and, as said before, the Nordbotten et al. (2005) solution and the Dentz and Tartakovsky (2009a) solution are used to achieve this purpose.

The validity of both solutions depends on the value of the gravity number defined in Eq. (4.3). The gravity number is a ratio of gravity to viscous forces and it is important to quantify the relative influence of buoyancy when we analyze the evolution of the CO<sub>2</sub> plume into the target aquifer:

$$N_g = \frac{k\Delta\rho g\bar{\rho}_c 2\pi r_c d}{\mu_c Q_m} \quad (4.3)$$

Where  $\Delta\rho$  is the difference between the fluids density,  $\bar{\rho}_c$  is a characteristic CO<sub>2</sub> density,  $r_c$  is a characteristic length,  $k$  is the aquifer permeability,  $g$  is the gravity,  $d$  is the thickness of the aquifer,  $Q_m$  is the CO<sub>2</sub> mass flow rate and  $\mu_c$  is the CO<sub>2</sub> viscosity.

In these four cases, gravity numbers are close to one (Table 4.1), which indicates that gravity and viscous forces are comparable. Therefore the interface position (Fig. 4.2-4.5) is similar to that of Nordbotten et al. (2005) in the lower half of the aquifer, where viscous forces may dominate, but it is similar to that of Dentz and Tartakovsky (2009a) in the upper part of the aquifer, where buoyancy begins to dominate.

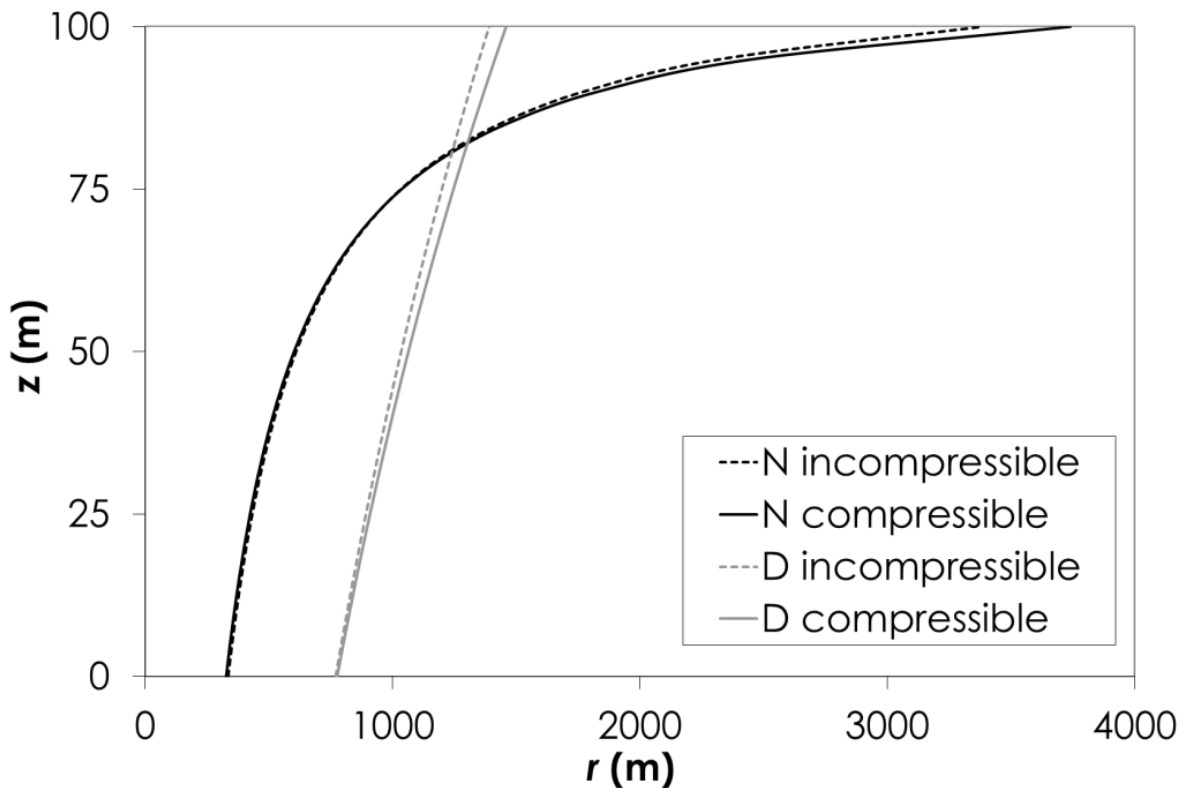


**Figure 4.2:** Abrupt interface position in a vertical cross section after 30 years of injection in the scenario 1. N means Nordbotten solution and D means Dentz and Tartakovsky solution.

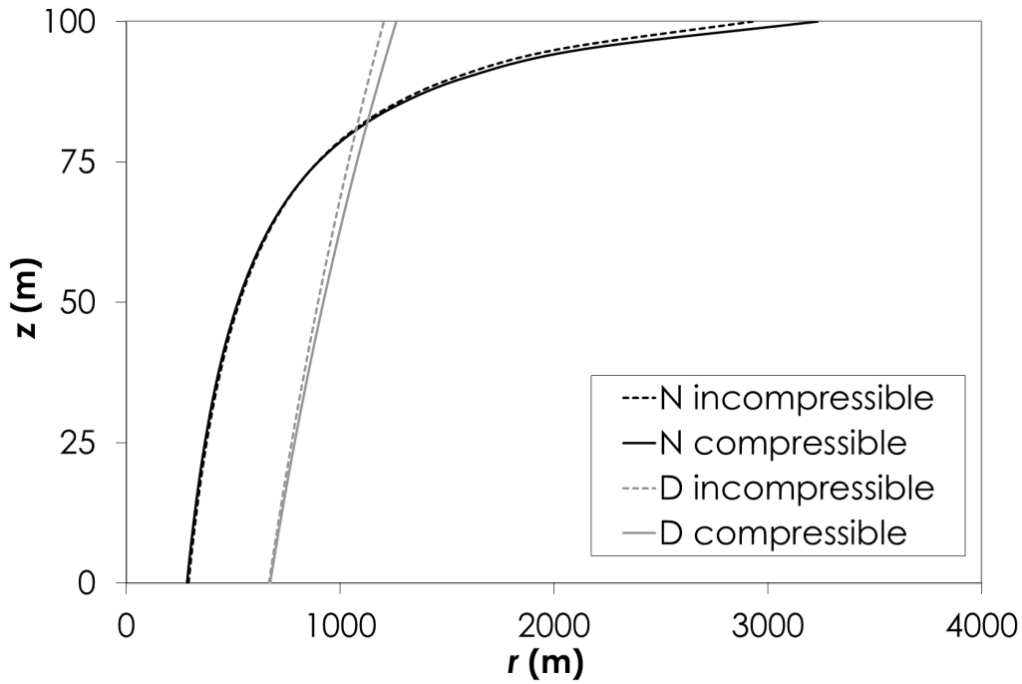


**Figure 4.3:** Abrupt interface position in a vertical cross section after 30 years of injection in the scenario 2. N means Nordbotten solution and D means Dentz and Tartakovsky solution.

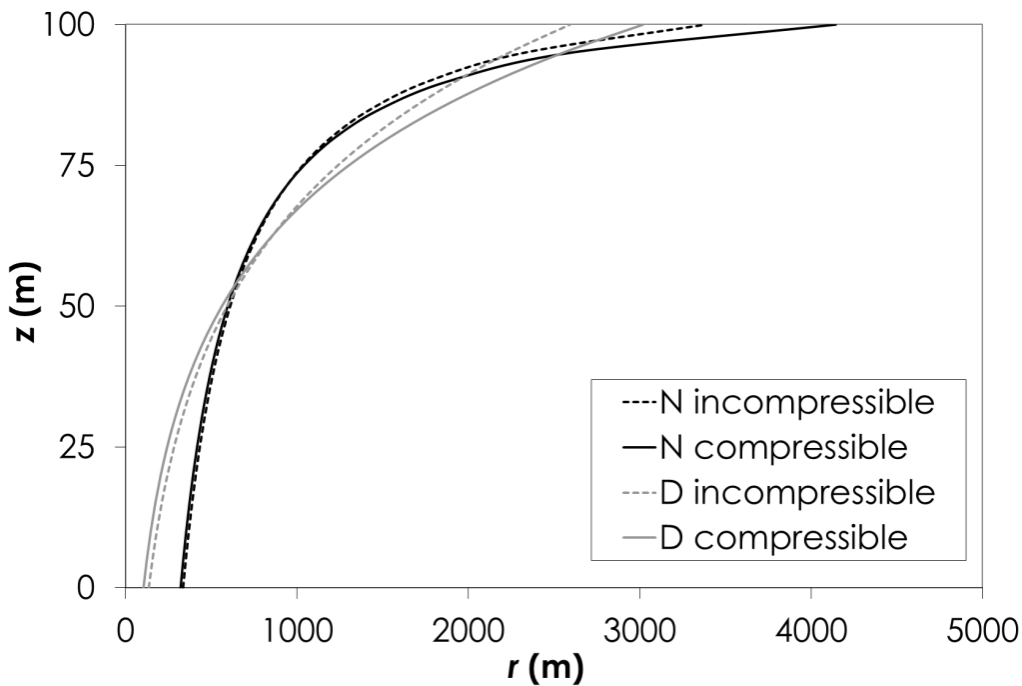


**Figure 4.4:** Abrupt interface position in a vertical cross section after 30 years of injection in the scenario 3. N means Nordbotten solution and D means Dentz and Tartakovsky solution.

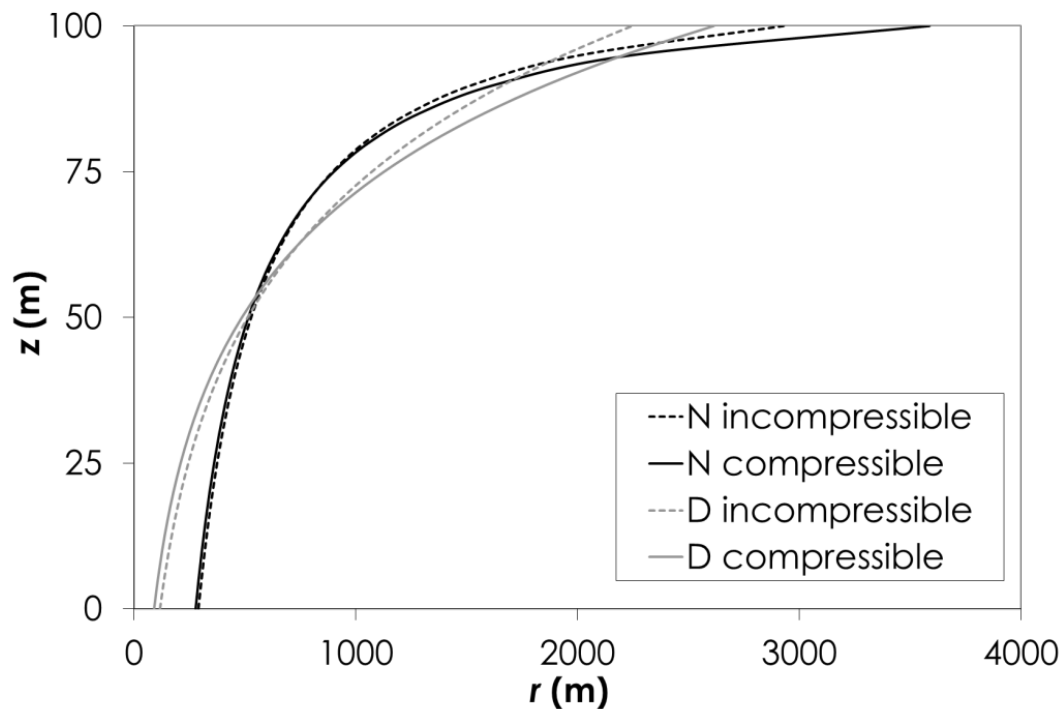


**Figure 4.5:** Abrupt interface position in a vertical cross section after 30 years of injection in the scenario 4. N means Nordbotten solution and D means Dentz and Tartakovsky solution.

The overpressure obtained with these methods is listed in Table 4.2 and it is calculated at a distance equal to the well radius (0.07 m). The difference between the results achieved with both solutions is negligible, nevertheless in our study we will use the maximum value of the resultant overpressures which represents the worst case. To calculate the total pressure, we suppose a hydrostatic pressure at the top of the aquifer of 10 MPa.

	$P_0$ (MPa)	$\Delta P_{Ni}$ (MPa)	$\Delta P_{Di}$ (MPa)	$\Delta P_{Final}$ (MPa)	$P_{Total}$ (MPa)
<b>Scenario 1</b>	10	3.11	3.35	3.35	13.35
<b>Scenario 2</b>	10	3.13	3.37	3.37	13.37
<b>Scenario 3</b>	10	1.15	1.31	1.31	11.31
<b>Scenario 4</b>	10	1.17	1.31	1.31	11.31

**Table 4.2:** Total pressure and overpressure considering only the effect of one well.

We now take into account the interference with other two injection wells 'j', at distance of 3 and 5 km respectively. The resultant overpressure ( $\sum_{j=1}^n \Delta P_{i \rightarrow j}$ ), calculated as explained in the foregoing (Eq. 4.2), is shown in Table 4.3, as well as the total overpressure obtained by the superposition with the overpressure generated by injection into the well 'i' (Eq. 4.1).

	<b>P<sub>0</sub></b> <b>(MPa)</b>	<b>ΔP<sub>Ni</sub></b> <b>(MPa)</b>	<b>ΔP<sub>Di</sub></b> <b>(MPa)</b>	<b>Σ<sub>j</sub>ΔP<sub>j</sub></b> <b>(MPa)</b>	<b>ΔP<sub>total</sub></b> <b>(MPa)</b>	<b>P<sub>total</sub></b> <b>(MPa)</b>
<b>Scenario 1</b>	10	3.11	3.35	3.67	7.02	17.02
<b>Scenario 2</b>	10	3.13	3.37	3.53	6.9	16.9
<b>Scenario 3</b>	10	1.15	1.31	0.95	2.26	12.26
<b>Scenario 4</b>	10	1.17	1.31	0.92	2.23	12.23

**Table 4.3:** Total pressure and overpressure considering the effect of the three wells.  $\Delta P_j$  is the overpressure generated by the other two wells 'j' in the study well 'i'.

The final overpressure significantly increases with respect to the values presented in Table 4.2. Therefore, it is very important to consider the interaction between wells if a multiple injection scenario is regarded, otherwise the expected cost as well as the expected behavior of the reservoir will be wrong.

Taking into account the reservoir properties used in this case study and the calculated overpressure, we determined the CO<sub>2</sub> storage cost using the FE/NETL CO<sub>2</sub> Saline Storage Cost Model (USDOE, 2014).

This model includes capital and operating costs for pumps, pipelines, injection wells, and monitoring wells and equipment. These costs are typically functions of key engineering parameters such as depth, pressure, and flow rate. Other cost elements are initial geological and geophysical (G&G) survey and regulatory costs for site selection, permitting and certification, and recurring non-well monitoring during the project injection period and afterwards. There are also cost parameters for contingencies and for general and administrative costs (a.k.a. owner's costs). Payments to the landowner for surface disturbance and injection rights are included as are "insurance payments" to a government entity that is assumed to take over long-term liability for the site after its abandonment. In particular, The FE/NETL CO<sub>2</sub> Saline Storage Cost Model is an Excel-based model that consists of four modules (Figure 4.6): Project Management, Geologic, Activity Cost, and Financial:

- Project Management Module: Site for project inputs that define the overall scope of the storage project and modeled outputs.
- Geologic Module: Site for geo-engineering equations, storage coefficients, geologic database; calculates injectivity and plume area for CO<sub>2</sub>. This module will also calculate water withdrawal

from CO<sub>2</sub> storage reservoir as well as subsequent treatment and disposal of water not rendered potable.

- Activity Cost Module: Site for cost database for all technology and labor used in a project; generates annual costs per technology/labor applied over life of storage project.
- Financial Module: Site that generates project financial statements and provides the project management sheet. Calculation of financial responsibility cost and cost of instruments to satisfy financial responsibility requirements are done within this module.

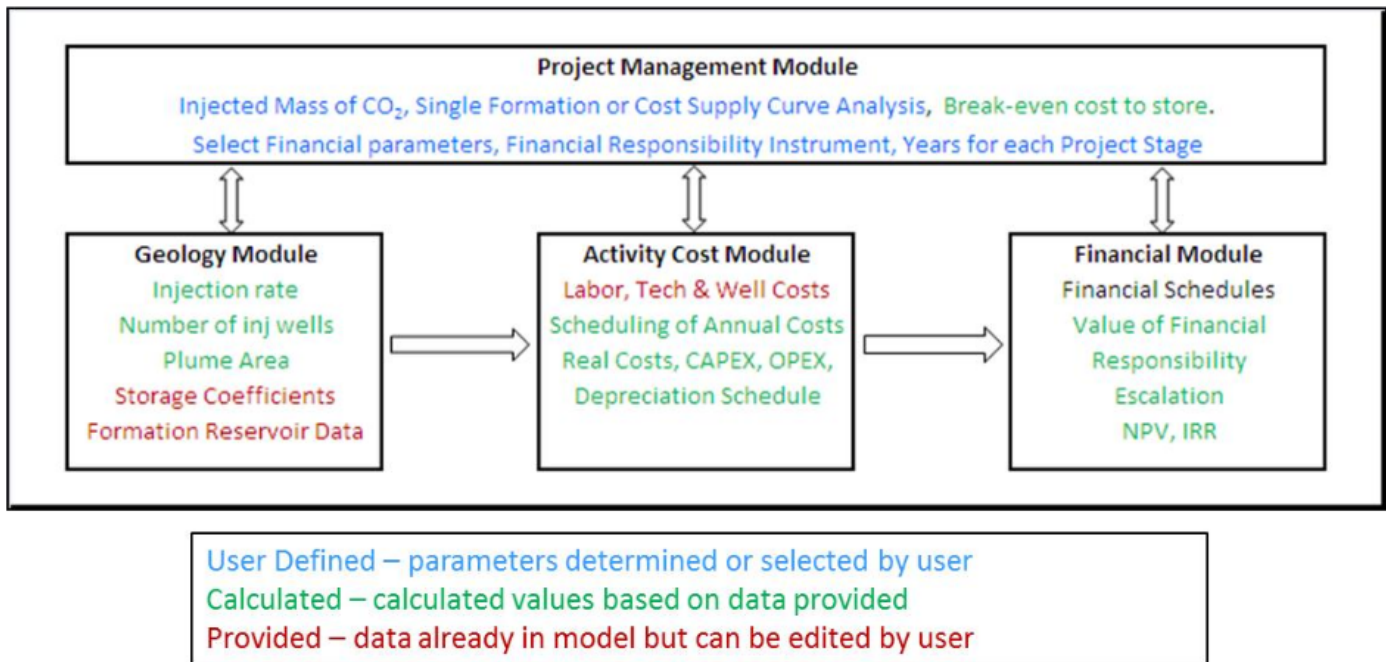


**Figure 4.5:** FE/NETL CO<sub>2</sub> saline storage cost model structure.

We calculated the CO<sub>2</sub> cost storage for the four cases studied here (Table 4.1) for a CO<sub>2</sub> injection of 3.2 Mt/yr through 3 different wells at a reservoir depth of 1 km at an initial pressure of 10MPa and temperature 40°C. The CO<sub>2</sub> injection is simulated during 30 years. We calculated the cost for two different CO<sub>2</sub> storage cost: one of 7.5\$/tCO<sub>2</sub> and another one with 15\$/tCO<sub>2</sub> to take into account an EOR scenario. We supposed that the pressure in the pipeline was equivalent to the higher injected pressure case corresponding to scenario with the lowest reservoir permeability. The results are presented in Table 4.4. We calculated the NPV (Net Present Value of project) and IRR (Internal rate of return for project) for the entire project and only for the CO<sub>2</sub> injection period without the previous reservoir characterization and wells perforation.

The reservoir geology used in the model is a clastic reservoir with fluvial deposit from cretaceous with an area of 100 km<sup>2</sup>.

The calculated NPV and IRR for the entire project presume that CO<sub>2</sub> injection start at year 7 of the project. The 3 first years are devoted to site characterization (2D and 3D seismic analysis, wells perforation, cores and fluid recovery) and the next two years are for permits obtaining before the operating step.

Parameters related to financing and fees are those used by NETL (2011). Monitoring and well related costs used in this study are those used by NETL (2014).

	\$/t <sub>CO2</sub>	NPV (\$)		IRR (%)		P <sub>out</sub> pipeline	P <sub>injection</sub>
		total	without previous characterization	total	without previous characterization	MPa	MPa
Scenario 1	7.5	-56437152	-15777965	-	-	13.1	13.1
Scenario 2	7.5	-30702589	989951	-	14.6	13.1	13.1
Scenario 3	7.5	-55993490	-15602933	-	-	13.1	11.1
Scenario 4	7.5	-29380752	2043158	-	17.2	13.1	11.1
Scenario 1	15	37113292	74590749	17.9	462.1	13.1	13.1
Scenario 2	15	66978320	99198629	23.3		13.1	13.1
Scenario 3	15	38442196	75800978	18.1	433.9	13.1	11.1
Scenario 4	15	68336706	100623939	23.5		13.1	11.1

**Table 4.4:** NPV and IRR for different CO<sub>2</sub> injection scenario.

We can observe in table 4.4, that in our case study the reservoir porosity is a key factor for the CO<sub>2</sub> storage costs whereas the reservoir permeability and thus the overpressure is not so important. In general, the case study is not a good candidate (reservoir thickness too thin) for CO<sub>2</sub> storage if no previous characterization has been done and no oil or gas recovery is available.

Nevertheless, if the reservoir is already well characterized, this reservoir is a good candidate for CO<sub>2</sub> storage and even more in case of EOR.

## 5. References

1. Alonso J, Navarro V, Calvo B, Asensio L. Hydro-mechanical analysis of CO<sub>2</sub> storage in porous rocks using a critical state model. *Int. J. Rock Mech. Min. Sci.* 2012; 54:19-26.
2. Barton N, Bandis S, Bakhtar K. Strength, deformation and conductivity coupling of rock joints. *Int. J. Rock Mech. Min. Sci. Geomech. Abstracts* 1985; 22 (3):121-40.
3. Bohnhoff M, Zoback MD, Chiaramonte L, Gerst JL, Gupta N. Seismic detection of CO<sub>2</sub> leakage along monitoring wellbores. *Int. J. Greenh. Gas Control* 2010; 4 (4):687-97.
4. Carbon Management Workshop, 2011. 9th Annual EOR Carbon Management Workshop, Houston, TX. Available at: <<http://www.co2conference.net>>.
5. Dentz, M., Tartakovsky, D.M.: Abrupt-interface solution for carbon dioxide injection into porous media. *Trans.Porous Media* 79, 15-27 (2009a)
6. Evans KF, Zappone A, Kraft T, Deichmann N, Moia F. A survey of the induced seismic responses to fluid injection in geothermal and CO<sub>2</sub> reservoirs in Europe. *Geothermics* 2012; 41:30-54.
7. Ferronato M, Gambolati G, Janna C, Teatini P. Geomechanical issues of anthropogenic CO<sub>2</sub> sequestration in exploited gas fields. *Energy Convers. Manage.* 2010; 51:1918-28.
8. GCCSI, 2011. Economic assessment of carbon capture and storage technologies: 2011 update, Prepared by Worley Parsons and Schlumberger, Global CCS Institute, Canberra, Australia
9. Goerke U-J, Park C-H, Wang W, Singh AK, Kolditz O. Numerical simulation of multiphase hydromechanical processes induced by CO<sub>2</sub> injection into deep saline aquifers. *Oil & Gas Sci. Tech.* 2011; 66:105-18.
10. Hsieh PA, Bredehoeft JD. A reservoir analysis of the Denver earthquakes: A case of induced seismicity. *J. Geophys. Res.* 1981; 86(B2):903-20.
11. IPCC Special Report on Carbon Dioxide Capture and Storage: Technical Summary, 2005.
12. International Energy Agency. Energy Technology Perspective. Scenarios and Strategies to 2050. 2010.
13. Mathias SA, Hardisty PE, Trudell MR, Zimmerman RW. Approximate solutions for pressure buildup during CO<sub>2</sub> injection in brine aquifers. *Transp. Porous Media* 2009; 79:269-84.
14. Joshi, S.D. Cost/Benefits of Horizontal Wells, SPE 83621, eastern Regional/AAPG Pacific Section Joint Meeting held in Long Beach, California, U.S.A., 19-24 May 2003.
15. Mathias SA, Gonzalez Martinez de Miguel GJ, Thatcher KE, Zimmerman RW. Pressure buildup during CO<sub>2</sub> injection into a closed brine aquifer. *Transp. Porous Media* 2011a; 89:383-97.

16. Mathias SA, Gluyas JG, Gonzalez Martinez de Miguel GJ, Hosseini SA. Role of partial miscibility on pressure buildup due to constant rate injection of CO<sub>2</sub> into closed and open brine aquifers. *Water Res. Res.* 2011b; 47, W12525, doi:10.1029/2011WR011051.
17. National Energy Technology Laboratory (NETL). Quality Guidelines for Energy System Studies: Cost Estimation Methodology for NETL Assessments of Power Plant Performance. DOE/NETL-2011/1455, Pittsburgh, PA.
18. National Energy Technology Laboratory (NETL). FE/NETL CO<sub>2</sub> Saline Storage Cost Model: Model Description and Baseline Results. DOE/NETL-2014/1659, Pittsburgh, PA.
19. Nordbotten, J.M., Celia, M.A., Bachu, S.: Injection and storage of CO<sub>2</sub> in deep saline aquifers: analytical solution for CO<sub>2</sub> plume evolution during injection. *Trans. Porous Media* 58, 339–360 (2005)
20. Rubin, E.S., Davison, J.E., Herzog, H.J. The cost of CO<sub>2</sub> capture and storage, *International Journal of Greenhouse gas control*, 40, 378-400, 2015.
21. Rutqvist J. The geomechanics of CO<sub>2</sub> storage in deep sedimentary formations. *Geotechn. Geol. Eng.* 2012; 30:525–51.
22. Rutqvist J, Tsang C-F. A study of caprock hydromechanical changes with CO<sub>2</sub> injection into a brine formation. *Environ. Geol.* 2002; 42:296–305.
23. Rutqvist J, Birkholzer JT, Tsang C-F. Coupled reservoir-geomechanical analysis of the potential for tensile and shear failure associated with CO<sub>2</sub> injection in multilayered reservoir-caprock systems. *Int. J. Rock Mech. Min. Sci.* 2008; 45:132-43.
24. de Simone S, Vilarrasa V, Carrera J, Alcolea A, Meier P. Thermal coupling may control mechanical stability of geothermal reservoirs during cold water injection. *Physics and Chemistry of the Earth* 2013; doi:10.1016/j.pce.2013.01.001.
25. Soltanzadeh H, Hawkes CD. Assessing fault reactivation tendency within and surrounding porous reservoirs during fluid production or injection. *Int. J. Rock Mech. Min. Sci.* 2009; 46:1-7.
26. Streit JE, Hillis RR. Estimating fault stability and sustainable fluid pressures for underground storage of CO<sub>2</sub> in porous rock. *Energy* 2004; 29:1445-56.
27. Suresh, B., 2010. *Che Marketing Research Report: Carbon Dioxide chemical economics handbook*. SRI Consulting.
28. Theis C. V., The relation between the lowering of the Piezometric surface and the rate and duration of discharge of a well using groundwater storage, *Eos, Transactions American Geophysical Union* 16.2 (1935) 519-524.
29. USDOE, 2014. FE/NETL CO<sub>2</sub> saline storage cost model: model description and baseline results, Report No. DOE/NETL-2014/1659, US Dept of Energy, National Energy Technology Laboratory, Pittsburgh, PA.
30. Verdon JP, Kendall J-M, White DJ, Angus DA. Linking microseismic event observations with geomechanical models to minimise the risks of storing CO<sub>2</sub> in geological formations. *Earth and Planetary Sci. Lett.* 2011; 305:143-52.

31. Vilarrasa V, Bolster D, Olivella S, Carrera J. Coupled hydromechanical modeling of CO<sub>2</sub> sequestration in deep saline aquifers. *Int. J. Greenh. Gas Control* 2010; 4 (6):910–19.
32. Vilarrasa V, Koyama T, Neretnieks I, Jing L. Shear-induced flow channels in a single rock fracture and their effect on solute transport. *Transp. Porous Media* 2011; 87(2):503–23.
33. Vilarrasa, V. Impact of CO<sub>2</sub> injection through horizontal and vertical wells on the caprock mechanical stability. *International Journal of Rock Mechanics and Mining Sciences*. 02/2014; 66:151–159. DOI: 10.1016/j.ijrmms.2014.01.001
34. Vilarrasa V, Bolster D, Dentz M, Olivella S, Carrera J. Effects of CO<sub>2</sub> Compressibility on CO<sub>2</sub> Storage in Deep Saline Aquifers. *Transp. Porous Media* 2010; 85:619–39.
35. Yeo IW, De Freitas MH, Zimmerman RW. Effect of shear displacement on the aperture and permeability of rock. *Int. J. Rock Mech. Min. Sci.* 1998; 35(8):1051–70.
36. ZEP (Zero Emissions Platform), 2011c. The costs of CO<sub>2</sub> storage: post-demonstration CCS in the EU, European Technology Platform for Zero Emission Fossil Fuel Power Plants, Brussels.
37. Zhang Z, Agarwal RK. Numerical simulation and optimization of CO<sub>2</sub> sequestration in saline aquifers for vertical and horizontal well injection. *Comput. Geosci.* 2012; 16:891–99.
38. Zhou Q, Birkholzer J, Tsang C-F, Rutqvist J. A method for quick assessment of CO<sub>2</sub> storage capacity in closed and semi-closed saline formations. *Int. J. Greenh. Gas Control* 2008; 2:626–39.